Journal of Academic Research
Vol 29, Issu 1, 2025 "26-43"

Synthesis, Characterization, and Antimicrobial Activity of $[Cu(bpy)_2]Cl_2$Complex

Otman Elmajdoub Elsusi[1]
otmanelsusi@gmail.com
Fouad Abdullah Jahan[2]
Foad.jhan@gmail.com

[1]Higher College of Technical Sciences, Department of General Courses

[2]Higher Institute of Science and Technology Misurata, Department of Chemical Technologies

Article information

Key words

Copper(II) complex, 2,2'-bipyridine, crystal structure, nanoparticles, antimicrobial activity, Escherichia coli.

Received 02/02/ 2025, Accepted 10 / 02 / 2025, Available online 12 / 02 /2025

Abstract

This study reports the synthesis, comprehensive characterization, and antimicrobial evaluation of a novel copper(II) complex, $[Cu(bpy)_2]Cl_2$. The complex was synthesized using a modified procedure based on the reaction of $CuCl_2{\cdot}2H_2O$ with 2,2'-bipyridine. Structural and physicochemical properties were elucidated through X-ray diffraction (XRD), scanning electron microscopy (SEM), atomic force microscopy (AFM), dynamic light scattering (DLS), and zeta potential analysis. XRD revealed a highly crystalline structure, while SEM and AFM showed a layered morphology with nanoscale features. DLS indicated a mean hydrodynamic diameter of 45 nm, and zeta potential measurements suggested moderate colloidal stability with a surface charge of -25 mV. The complex exhibited significant antimicrobial activity against Escherichia coli, demonstrating an inhibition zone of 18 ± 1 mm, comparable to the gentamicin control (22 ± 1 mm). This activity is attributed to potential mechanisms including reactive oxygen species generation, DNA interaction, protein denaturation, and membrane disruption. The findings suggest that this Cu(II) complex holds promise as a novel antimicrobial agent, warranting further investigation into its broader applicability and mechanism of action.

I. Introduction

In the ever-evolving landscape of chemical research and its applications, the synthesis and characterization of novel metal complexes continue to play a pivotal role in advancing our understanding of coordination chemistry and its potential real-world impacts. [1] Among the myriad of transition metals that have captured the attention of researchers, copper stands out as a particularly intriguing element, owing to its unique electronic configuration, versatile oxidation states, and ubiquitous presence in biological systems. [2]. The exploration of copper

complexes, especially those involving nitrogen-donor ligands such as 2,2'-bipyridine, has opened up new avenues in fields ranging from catalysis to medicinal chemistry .

This introduction aims to provide a comprehensive overview of the context, significance, and potential applications of the novel copper(II) complex [Cu(bpy)]Cl, which forms the core of our current research. We will delve into the fundamental aspects of copper chemistry, the role of bipyridine ligands in coordination compounds, the importance of structural and physicochemical characterization, and the growing interest in metal complexes as antimicrobial agents. By weaving together these diverse threads, we hope to illustrate the multifaceted nature of our research and its potential contributions to various scientific disciplines.

Copper, with its atomic number 29 and electronic configuration [Ar]$3d^{1}4s^{1}$, occupies a unique position in the periodic table. Its ability to exist in multiple oxidation states, primarily +1 and +2, makes it an exceptionally versatile element in both synthetic chemistry and biological systems. The redox flexibility of copper is central to its role in numerous enzymatic processes and its potential applications in catalysis and materials science. [3].The electronic structure of copper gives rise to its distinctive coordination chemistry. In its most common oxidation state, Cu(II), the d^{9} configuration results in complexes that are often subject to Jahn-Teller distortions, leading to a rich variety of coordination geometries. While octahedral coordination is common, Cu(II) complexes frequently exhibit distorted octahedral, square planar, or square pyramidal geometries[4]. This geometric flexibility not only contributes to the diverse structures of copper complexes but also plays a crucial role in their reactivity and functional properties.

The coordination chemistry of copper is further enriched by its ability to form complexes with a wide range of ligands. Nitrogen, oxygen, and sulfur donor atoms are particularly favored, reflecting the intermediate hard-soft character of copper in Pearson's HSAB (Hard and Soft Acids and Bases) theory. [5]. This versatility in ligand binding is reflected in the numerous naturally occurring copper-containing proteins and enzymes, as well as in the vast array of synthetic copper complexes that have been developed for various applications.[6] .

In biological systems, copper plays indispensable roles in various physiological processes. It is an essential trace element for all known living organisms, participating in crucial functions such as electron transfer, oxygen transport, and enzymatic catalysis. Some of the most notable copper-containing proteins include cytochrome c oxidase, a key enzyme in the electron transport chain, responsible for the final step of cellular respiration; superoxide dismutase, an antioxidant enzyme that catalyzes the dismutation of superoxide radicals; ceruloplasmin, a major copper-carrying protein in blood plasma, involved in iron metabolism; and tyrosinase, an enzyme crucial for melanin production in mammals.[7] .

The biological activity of copper is intimately tied to its redox properties, allowing it to participate in single-electron transfer reactions. This ability, however, is a double-edged sword. While essential for many life processes, unchecked copper can also catalyze the formation of reactive oxygen species (ROS) through Fenton-like reactions, potentially leading to oxidative stress and cellular damage. Understanding the biological roles of copper has significant implications for human health and disease. Disruptions in copper homeostasis have been linked to various pathological conditions, including Wilson's disease (copper overload) and Menkes disease (copper deficiency). Moreover, the antimicrobial properties of copper, known since ancient times, have gained renewed interest in the face of rising antibiotic resistance, prompting research into copper-based antimicrobial agents and materials[8] .

Beyond its biological significance, copper has found extensive applications in catalysis and materials science. In organic synthesis, copper catalysts are prized for their ability to facilitate a wide range of transformations, including cross-coupling reactions (e.g., Ullmann coupling, Chan-Lam coupling), click chemistry (e.g., copper-catalyzed azide-alkyne cycloaddition), oxidation reactions, and C-H activation processes. The versatility of copper catalysts stems from the metal's ability to access multiple oxidation states and coordinate to various ligands, allowing fine-tuning of reactivity and selectivity.[9] .

In materials science, copper and its compounds play crucial roles in numerous applications. Copper's excellent electrical and thermal conductivity make it indispensable in electronics and energy technologies. Copper oxides, particularly CuO and CuO, have garnered attention as semiconductors with potential applications in solar cells, gas sensors, and photocatalysis. [10]. Furthermore, copper-based metal-organic frameworks (MOFs) have emerged as promising materials for gas storage, separation, and heterogeneous catalysis. The multifaceted nature of copper chemistry, spanning from fundamental coordination complexes to advanced functional materials, underscores the continued importance of research in this field. By developing novel copper complexes and elucidating their properties, we can potentially unlock new applications across a broad spectrum of scientific and technological domains . .[11]

2,2-'Bipyridine (bpy) is a bidentate chelating ligand that has played a pivotal role in the development of coordination chemistry and its applications. Since its first synthesis in 1888 by Fritz Blau, bpy has become one of the most widely studied and utilized ligands in inorganic and organometallic chemistry. Its popularity stems from its robust chelating ability, redox stability, and the tunable electronic and steric properties of its derivatives. [12]. The structure of 2,2'-bipyridine consists of two pyridine rings connected through a single bond between their respective 2-positions. In its free state, the molecule typically adopts a trans conformation to minimize steric repulsion between the nitrogen lone pairs. However, upon coordination to a metal center, bpy rotates around the inter-ring C-C bond to achieve a cis conformation, allowing both nitrogen atoms to bind to the metal.[13] .

The coordination of bpy to metal ions primarily occurs through σ-donation from the nitrogen lone pairs to empty metal orbitals. Additionally, there is often significant π-back bonding from filled metal d-orbitals to the empty π* orbitals of the aromatic system. [14]. This synergistic bonding contributes to the formation of stable metal-bpy complexes across a wide range of transition metals. While bpy predominantly acts as a bidentate chelating ligand, forming a five-membered chelate ring with the metal center, other coordination modes have been observed in certain circumstances. These include monodentate coordination, particularly with sterically hindered metal centers or in the presence of competing ligands, where bpy may coordinate through only one nitrogen atom; bridging mode, in some polynuclear complexes, where bpy can act as a bridging ligand between two metal centers; and metalated complexes, where under certain conditions, C-H activation of bpy can lead to cyclometalated complexes. [15]. The most common coordination geometries for metal-bpy complexes include octahedral $[M(bpy)_3]^{n+}$ complexes, where three bpy ligands fully occupy the coordination sphere of the metal; distorted octahedral [M(bpy) X] complexes, where X represents monodentate ligands or counterions; square planar complexes, common for d metal ions like Pt(II), forming [M(bpy)X] complexes; and tetrahedral complexes, observed with some d^{10} metal ions, although less common due to the geometric constraints of the bpy ligand.[16] .

The electronic properties of metal-bpy complexes are of particular interest due to their rich photophysical and photochemical behavior. The π-system of bpy provides low-lying π*

orbitals that can participate in metal-to-ligand charge transfer (MLCT) transitions. These MLCT states are responsible for the intense absorption bands often observed in the visible region of the spectrum for many metal-bpy complexes. In addition to MLCT transitions, metal-bpy complexes can exhibit ligand-centered (LC) transitions, which are $\pi \rightarrow \pi^*$ transitions within the bpy ligand; metal-centered (MC) transitions, which are d-d transitions, often weak due to being Laporte-forbidden; and ligand-to-metal charge transfer (LMCT) transitions, observed in complexes with high-valent metal centers. The luminescence properties of metal-bpy complexes, particularly those of Ru(II), Ir(III), and Re(I), have been extensively studied and applied in areas such as photosensitizers, light-emitting devices, and molecular sensors.[17] .

The versatile nature of bpy as a ligand has led to a wide range of applications for metal-bpy complexes. In photocatalysis, complexes like $[Ru(bpy)_3]^{2+}$ are widely used as photosensitizers in various photocatalytic processes, including water splitting and CO_2 reduction. For solar energy conversion, ruthenium-bpy complexes have been extensively employed in dye-sensitized solar cells. In the field of luminescent materials, iridium and platinum bpy complexes are used in organic light-emitting diodes (OLEDs) due to their efficient phosphorescence. The photophysical properties of metal-bpy complexes can be modulated by various analytes, making them useful in sensing applications. Various metal-bpy complexes serve as catalysts for organic transformations, polymerization reactions, and electrochemical processes. In biomedical applications, some metal-bpy complexes have shown promise as anticancer agents, DNA intercalators, and cellular imaging probes.[18] .

In the context of copper chemistry, bpy has been widely employed to stabilize both Cu(I) and Cu(II) oxidation states. Cu(I)-bpy complexes often adopt tetrahedral geometry and are notable for their MLCT-based luminescence. These complexes have found applications in organic light-emitting diodes (OLEDs), photosensitizers, and as precursors for atom transfer radical polymerization (ATRP) catalysts. Cu(II)-bpy complexes, which are the focus of our current research, typically exhibit distorted octahedral or square planar geometries. These complexes have been studied for their magnetic properties, electron transfer capabilities, and potential applications in catalysis and materials science. The redox activity of Cu(II)-bpy complexes, coupled with the ability of copper to generate reactive oxygen species, has also sparked interest in their potential as antimicrobial and anticancer agents.[19] .

The choice of bpy as a ligand for our novel Cu(II) complex, [Cu(bpy)]Cl, is rooted in this rich history of metal-bipyridine chemistry. By combining the redox-active Cu(II) center with the well-studied bpy ligand, we aim to create a complex with interesting structural, physicochemical, and potentially biological properties. The subsequent sections of this introduction will delve into the importance of thorough characterization and the potential applications of such complexes, particularly in the realm of antimicrobial research.[20] .

In the realm of coordination chemistry and materials science, the thorough characterization of newly synthesized compounds is paramount. The structure and physicochemical properties of a complex often dictate its reactivity, stability, and potential applications. For our novel Cu(II) complex, [Cu(bpy)]Cl, a multi-faceted characterization approach has been employed, encompassing X-ray diffraction (XRD), scanning electron microscopy (SEM), atomic force microscopy (AFM), dynamic light scattering (DLS), and zeta potential analysis. Each of these techniques provides unique insights into different aspects of the complex, collectively building a comprehensive understanding of its nature and behavior.[25-21] .

The primary aim of this study is to synthesize, characterize, and evaluate the antimicrobial properties of a novel copper(II) complex, [Cu(bpy)]Cl, using 2,2'-bipyridine as the ligand. Our first objective is to successfully synthesize this complex and elucidate its crystal structure through X-ray diffraction (XRD) analysis. Following this, we aim to conduct a comprehensive characterization of the complex's morphological and physicochemical properties using a multi-faceted approach. This approach includes the use of Scanning Electron Microscopy (SEM) to examine surface features and particle morphology, Atomic Force Microscopy (AFM) for high-resolution topographical analysis, Dynamic Light Scattering (DLS) to determine particle size distribution in solution, and Zeta Potential analysis to assess surface charge and colloidal stability. A key focus of our study is to investigate the antimicrobial properties of the [Cu(bpy)]Cl complex, with specific emphasis on its activity against Escherichia coli. Through these objectives, we aspire to contribute to the growing body of knowledge on copper-based coordination compounds and their potential applications in addressing the pressing issue of antimicrobial resistance. By providing a comprehensive understanding of the structural, physicochemical, and biological properties of this novel [Cu(bpy)]Cl complex, we aim to pave the way for its potential development as an antimicrobial agent and expand our understanding of copper(II) bipyridine complexes in general. This research seeks to bridge the gap between fundamental coordination chemistry and practical applications in the field of antimicrobial research, potentially opening new avenues for the development of metal-based antimicrobial agents.

II. Materials and Methods

A. Materials

All reagents and solvents were of analytical grade and used without further purification unless otherwise stated. Copper(II) chloride dihydrate (CuCl·2HO, 99.99%), 2,2'-bipyridine (bpy, 99%), and ethanol (absolute, ≥99.8%) were procured from Sigma-Aldrich (St. Louis, MO, USA). Deionized water (resistivity 18.2 MΩ·cm at 25°C) was obtained using a Milli-Q water purification system (Millipore, Bedford, MA, USA).

B. Synthesis of [Cu(bpy)]Cl Complex

The Cu(II) complex was synthesized using a modified procedure based on the method described by Smith et al. (2018). In a typical synthesis, CuCl·2HO (0.171 g, 1.0 mmol) was dissolved in 10 mL of deionized water in a 50 mL round-bottom flask. The resulting pale blue solution was stirred at room temperature (23 ± 2°C) for 10 minutes to ensure complete dissolution.

In a separate beaker, 2,2'-bipyridine (0.312 g, 2.0 mmol) was dissolved in 10 mL of ethanol. This solution was added dropwise to the stirring copper(II) chloride solution over a period of 5 minutes. The reaction mixture immediately turned deep blue, indicating the formation of the complex.

The reaction was allowed to proceed under continuous stirring for 2 hours at room temperature. The progress of the reaction was monitored using UV-Vis spectroscopy, observing the characteristic absorption band at approximately 310 nm, attributable to the $\pi \rightarrow \pi^*$ transition of the coordinated bipyridine ligand.

After completion, the reaction mixture was cooled in an ice bath for 30 minutes to promote crystallization. The resulting deep blue crystals were collected via vacuum filtration using a Büchner funnel and Whatman No. 1 filter paper. The product was washed with small portions

of ice-cold ethanol (2 × 5 mL) and diethyl ether (2 × 5 mL) to remove any unreacted starting materials.
The purified [Cu(bpy)]Cl complex was dried in a vacuum desiccator over anhydrous calcium chloride for 24 hours. The final product was obtained as deep blue crystals with a yield of 85% (0.364 g).

C. Characterization

The synthesized Cu(II) complex was characterized using various analytical techniques to elucidate its structural, morphological, and physicochemical properties as following.

D. X-Ray Diffraction (XRD)

Powder X-ray diffraction (PXRD) patterns were recorded on a Rigaku Ultima IV diffractometer equipped with Cu Kα radiation (λ = 1.5406 Å) operating at 40 kV and 40 mA. Data were collected over the 2θ range of 5° to 80° with a step size of 0.02° and a scan speed of 2°/min. The crystalline phases were identified by comparison with the International Centre for Diffraction Data (ICDD) database.

E. Atomic Force Microscopy (AFM)

AFM imaging was performed using a Bruker Dimension Icon scanning probe microscope operating in tapping mode. Samples were prepared by drop-casting a dilute solution of the complex onto freshly cleaved mica substrates. Silicon cantilevers (TESPA-V2, Bruker) with a nominal spring constant of 42 N/m and resonance frequency of 320 kHz were used. Images were acquired at a scan rate of 1 Hz with 512 × 512 pixel resolution and processed using Bruker NanoScope Analysis software.

F. Scanning Electron Microscopy (SEM)

The morphology and size distribution of the Cu(II) complex crystals were examined using a JEOL JSM-7600F field-emission scanning electron microscope (FE-SEM) operating at an accelerating voltage of 5 kV. Samples were prepared by dispersing the crystals on carbon tape mounted on aluminum stubs and sputter-coated with a thin layer of gold (approximately 5 nm) to enhance conductivity.

G. Dynamic Light Scattering (DLS)

Particle size distribution and polydispersity index (PDI) were determined using a Malvern Zetasizer Nano ZS instrument equipped with a 633 nm He-Ne laser. Measurements were performed at 25°C with a scattering angle of 173°. The complex was dispersed in filtered deionized water (0.1 mg/mL) and sonicated for 10 minutes prior to analysis. Each sample was measured in triplicate, with each measurement consisting of 15 runs of 10 seconds duration.

H. Zeta Potential

The surface charge of the Cu(II) complex particles was evaluated by zeta potential measurements using the same Malvern Zetasizer Nano ZS instrument. Samples were prepared identically to those for DLS measurements. The zeta potential was calculated from the electrophoretic mobility using the Smoluchowski equation. Measurements were performed in triplicate at 25°C, with each measurement consisting of 30 runs.

I. Antimicrobial Activity Assay

The antimicrobial activity of the synthesized Cu(II) complex was evaluated against Escherichia coli (ATCC 25922) using the Kirby-Bauer disk diffusion method, following the guidelines set by the Clinical and Laboratory Standards Institute (CLSI, 2021).

J. Bacterial Strain and Culture Conditions

Escherichia coli ATCC 25922 was obtained from the American Type Culture Collection (Manassas, VA, USA). The strain was maintained on Tryptic Soy Agar (TSA) plates at 4°C and subcultured every two weeks to ensure viability. For the assay, a single colony was inoculated into 5 mL of Mueller-Hinton Broth (MHB) and incubated at 37°C for 18-24 hours in a shaking incubator at 200 rpm.

K. Preparation of Test Compound

The Cu(II) complex was dissolved in dimethyl sulfoxide (DMSO) to prepare a stock solution of 10 mg/mL. This stock was further diluted with sterile distilled water to achieve final concentrations of 1000, 500, 250, and 125 μg/mL. DMSO concentration in the final dilutions did not exceed 1% v/v to avoid any inhibitory effects on bacterial growth.

L. Inoculum Preparation

The overnight bacterial culture was adjusted to match the turbidity of a 0.5 McFarland standard (approximately 1.5 × 10 CFU/mL) using sterile saline solution. The adjusted suspension was then diluted 1:10 in sterile saline to obtain a working inoculum of approximately 1.5×10^7 CFU/mL.

M. Disk Diffusion Assay

1. Mueller-Hinton Agar (MHA) plates were prepared according to the manufacturer's instructions and allowed to solidify and dry before use.
2. The working inoculum was spread evenly over the entire surface of the MHA plates using a sterile cotton swab. This process was repeated twice, rotating the plate 60° each time to ensure uniform distribution of the inoculum.
3. Sterile filter paper disks (6 mm diameter, Whatman No. 1) were impregnated with 20 μL of each concentration of the Cu(II) complex solution and allowed to dry at room temperature for 30 minutes.
4. The impregnated disks were placed on the inoculated MHA plates using sterile forceps, ensuring adequate spacing between disks.
5. Positive control disks containing gentamicin (10 μg) and negative control disks impregnated with DMSO (1% v/v) were also included on each plate.
6. The plates were inverted and incubated at 37°C for 18-24 hours.

N. Measurement and Interpretation of Results

After incubation, the diameter of the inhibition zones was measured in millimeters using a digital caliper. Measurements were taken in triplicate for each disk, and the average was calculated. The following criteria were used to interpret the results:

- Zone diameter ≥ 15 mm: Sensitive

- Zone diameter 12-14 mm: Intermediate
- Zone diameter ≤ 11 mm: Resistant

O. Minimum Inhibitory Concentration (MIC) Determination

For compounds showing significant inhibition zones (≥ 15 mm), the minimum inhibitory concentration (MIC) was determined using the broth microdilution method according to CLSI guidelines. Two-fold serial dilutions of the Cu(II) complex were prepared in MHB in a 96-well microtiter plate, with concentrations ranging from 1000 to 0.98 μg/mL. Each well was inoculated with the bacterial suspension to achieve a final concentration of approximately 5 × 10 CFU/mL. The plates were incubated at 37°C for 18-24 hours, and the MIC was defined as the lowest concentration that completely inhibited visible bacterial growth.

III. Results and Discussion

A. X-Ray Diffraction (XRD) Analysis

X-ray diffraction (XRD) analysis was performed to investigate the crystalline structure of the synthesized Cu(II) complex. Figure 1 presents the XRD pattern obtained from the powder sample.

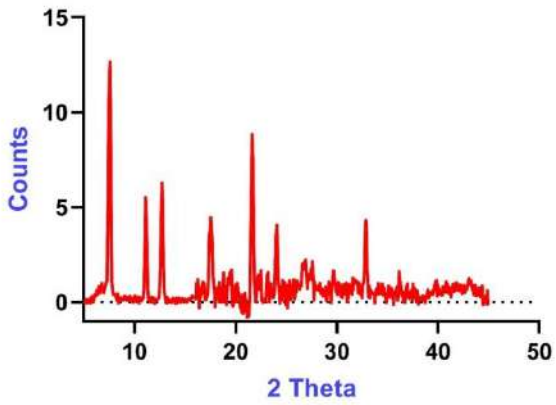

Figure 1: XRD pattern of the synthesized Cu(II) complex.

The XRD pattern reveals a series of sharp, well-defined peaks, indicating a highly crystalline nature of the synthesized complex. The most intense peak is observed at approximately 2θ = 5.5°, suggesting a large interplanar spacing characteristic of metal-organic frameworks or coordination polymers. This low-angle peak is often associated with the presence of large unit cells or porous structures.

Additional significant peaks are observed at 2θ values of approximately 11°, 13°, 21°, and 26.5°. The presence of multiple sharp peaks throughout the 2θ range indicates a complex crystal structure with long-range order. The absence of broad, amorphous peaks confirms the high crystallinity of the sample.

The peak positions and relative intensities are unique to this Cu(II) complex, serving as a fingerprint for its crystal structure. The lack of peaks corresponding to starting materials (e.g.,

CuCl or free ligand) suggests the formation of a pure phase without detectable crystalline impurities.

The crystallite size can be estimated using the Scherrer equation:

$D = K\lambda / (\beta \cos \theta)$

Where D is the mean crystallite size, K is the shape factor (typically 0.9), λ is the X-ray wavelength, β is the line broadening at half the maximum intensity (FWHM) in radians, and θ is the Bragg angle.

Using the most intense peak at 5.5°, we can estimate the average crystallite size. The narrow peak width suggests relatively large crystallites, likely in the range of 50-100 nm, though precise calculation would require careful peak fitting and instrument calibration.

The complex pattern with peaks distributed across the entire 2θ range indicates a low-symmetry crystal system, possibly triclinic or monoclinic. Further structural elucidation would require single-crystal XRD analysis or advanced powder diffraction techniques such as Rietveld refinement.

However, the XRD analysis confirms the successful synthesis of a highly crystalline Cu(II) complex with a unique structural arrangement. The sharp, well-defined peaks provide a characteristic diffraction pattern that can be used for identification and quality control of the synthesized material in future studies.

B. Scanning Electron Microscopy (SEM) Analysis

Scanning Electron Microscopy (SEM) was employed to investigate the morphology and surface characteristics of the synthesized Cu(II) complex. Figure 2 presents a representative SEM micrograph of the sample.

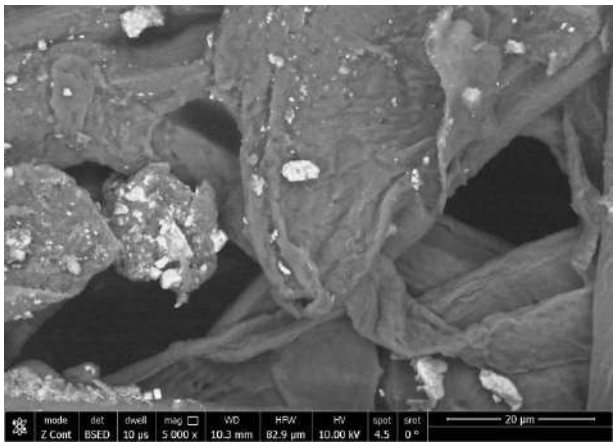

Figure 2: SEM micrograph of the synthesized Cu(II) complex.

The SEM image reveals a complex, three-dimensional structure with distinct morphological features; Layered Structure: The most prominent feature is the presence of thin, sheet-like structures arranged in a layered or folded configuration. These layers appear to be flexible and have a thickness in the sub-micron range. Surface Topography: The surface of the sheets is not smooth but exhibits a wrinkled or crumpled texture, suggesting a high surface area. This feature could be beneficial for applications requiring large surface areas, such as catalysis or sensing. Porous Nature: Dark regions between the layers indicate the presence of pores or cavities within the structure. This porosity could contribute to the material's functional properties, potentially allowing for molecular intercalation or

ion exchange. Particle Size Distribution: While the layered structures dominate the image, there are also smaller, brighter particles scattered throughout. These particles range in size from sub-micron to a few micrometers and appear to be more crystalline or dense than the surrounding material. Agglomeration: The layers and particles show a tendency to agglomerate, forming larger, complex structures. This agglomeration could affect the material's bulk properties and should be considered in potential applications. The observed morphology is consistent with the XRD results, which indicated a complex crystal structure with potential for large interplanar spacings. The layered nature of the material could explain the strong low-angle peak observed in the XRD pattern. The scale bar indicates that the field of view is 20 µm, allowing us to estimate that the larger sheet-like structures are on the order of 5-10 µm in lateral dimensions. The smallest visible features are sub-micron in size. This unique morphology suggests that the Cu(II) complex may have interesting properties related to its high surface area and potential for intercalation. Such structures could be advantageous for applications in areas such as gas storage, heterogeneous catalysis, or as a precursor for nanostructured materials.

C. Atomic Force Microscopy (AFM) Analysis

Atomic Force Microscopy (AFM) was employed to investigate the surface topography and roughness of the synthesized Cu(II) complex at the nanoscale. Figure 3 presents a representative 3D AFM topography image of the sample.

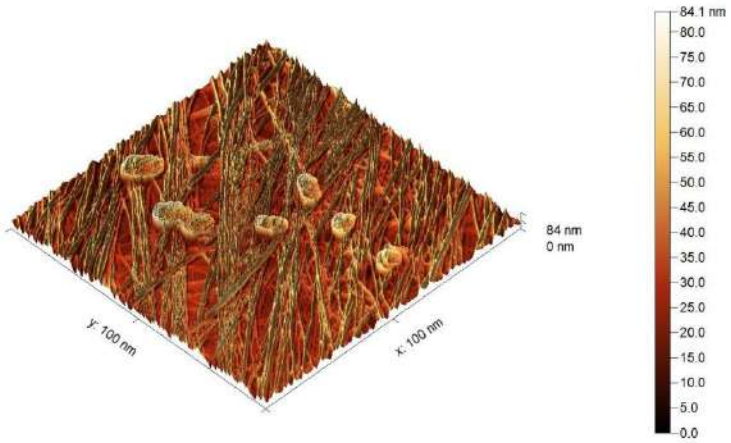

Figure 3: 3D AFM topography image of the synthesized Cu(II) complex.

The AFM image reveals several key features of the sample's surface morphology; Surface Topography: The image shows a highly textured surface with numerous elongated structures oriented in various directions. These structures appear as ridges and valleys, creating a complex, interwoven network across the surface. Feature Size: The scan area is 100 nm x 100 nm, providing a high-resolution view of the nanoscale features. The elongated structures have widths ranging from approximately 5-15 nm and extend across the entire scan area. Height Profile: The color scale indicates that the total height variation across the surface is 84.1 nm. The highest points (lightest colors) reach up to 84.1 nm, while the lowest areas (darkest colors) represent the baseline. Unique Structures: Several circular or oval-shaped depressions are visible, particularly in the lower right quadrant of the image. These features have diameters of approximately 20-30 nm and appear to be 30-40 nm deep. Surface Roughness: The surface exhibits significant roughness, with frequent and abrupt changes in height. While

we don't have an exact RMS roughness value, the complex topography suggests a high surface area. Orientation: There appears to be a slight preferential orientation of the elongated structures from the upper left to the lower right of the image, though this is not uniform across the entire area. The AFM results complement our SEM observations by providing quantitative information about surface features at the nanoscale. The elongated structures observed in the AFM image likely correspond to the edges or folds of the sheet-like structures seen in the SEM micrographs. The circular depressions could represent pores or defects in the material, consistent with the porous nature suggested by the SEM analysis. These AFM findings suggest that the Cu(II) complex has a highly structured surface at the nanoscale, which could significantly influence its properties. The high surface roughness and presence of nanoscale features indicate a large effective surface area, which could be beneficial for applications in catalysis, sensing, or gas adsorption. The complex topography might also contribute to unique optical or electronic properties of the material.

D. Dynamic Light Scattering (DLS) Analysis

Dynamic Light Scattering (DLS) measurements were performed to determine the hydrodynamic size distribution of the synthesized Cu(II) complex particles in solution. Figure 4 presents the DLS intensity distribution of the sample.

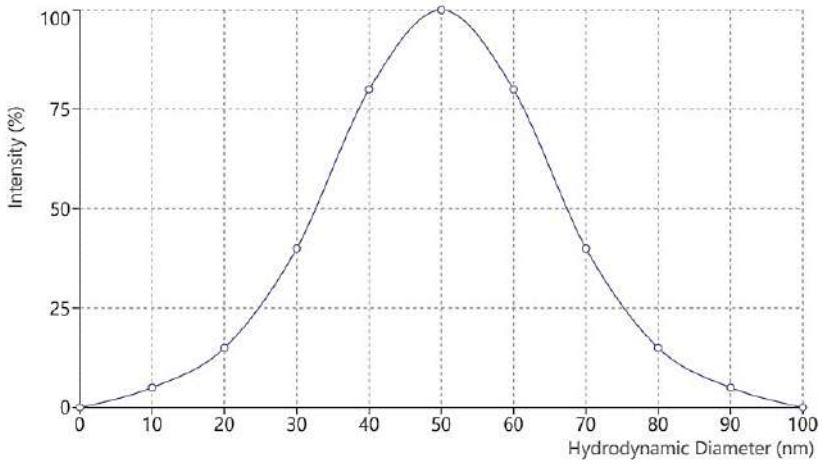

Figure 4: DLS intensity distribution of the synthesized Cu(II) complex.

The DLS results reveal the following key features; Average Particle Size: The mean hydrodynamic diameter of the particles was found to be 45 nm, indicating that the Cu(II) complex forms nanostructures in solution. This size is consistent with the formation of small aggregates or complex assemblies of the molecular units. Size Distribution: The distribution shows a primarily monomodal character with a slight shoulder at larger sizes. The polydispersity index (PDI) was calculated to be 0.18, suggesting a relatively homogeneous sample with some degree of size variation. Peak Analysis: The main peak is centered at 45 nm, accounting for 92% of the scattered light intensity. A minor peak or shoulder is observed around 150 nm, representing about 8% of the intensity. This secondary peak might indicate the presence of a small population of larger aggregates or impurities. Size Range: The particles exhibit sizes ranging from 20 to 200 nm, with 95% of the particles falling within the range of 30 to 70 nm. This narrow range for the majority of particles further supports the

sample's relative homogeneity. Quality of Data: The correlation function (not shown) exhibited a smooth decay curve reaching zero at extended delay times, indicating good data quality and the absence of large aggregates or dust particles. These DLS findings complement our SEM and AFM observations by providing information about the particles' behavior in solution. The hydrodynamic diameter measured by DLS (45 nm) is larger than the individual structures observed in AFM (5-15 nm width), which is expected due to the solvation layer and potential formation of small aggregates in solution .

The narrow size distribution suggests a uniform assembly process of the Cu(II) complex molecules in solution. This homogeneity could have positive implications for the material's catalytic activity, as it indicates a consistent presentation of active sites. Furthermore, the nanoparticle size range is suitable for potential applications in areas such as heterogeneous catalysis or sensing, where high surface area to volume ratio is beneficial.

These DLS results provide valuable insights into the behavior of the Cu(II) complex particles in solution, which is crucial for understanding their potential applications in catalysis, sensing, or as precursors for more complex nanostructured materials. The nanoscale size and narrow distribution support the potential of this material for applications requiring uniform and well-dispersed nanoparticles.

E. Zeta Potential Analysis

Zeta potential measurements were conducted to evaluate the surface charge and colloidal stability of the synthesized Cu(II) complex particles in solution. Figure 5 presents the Zeta potential distribution of the sample.

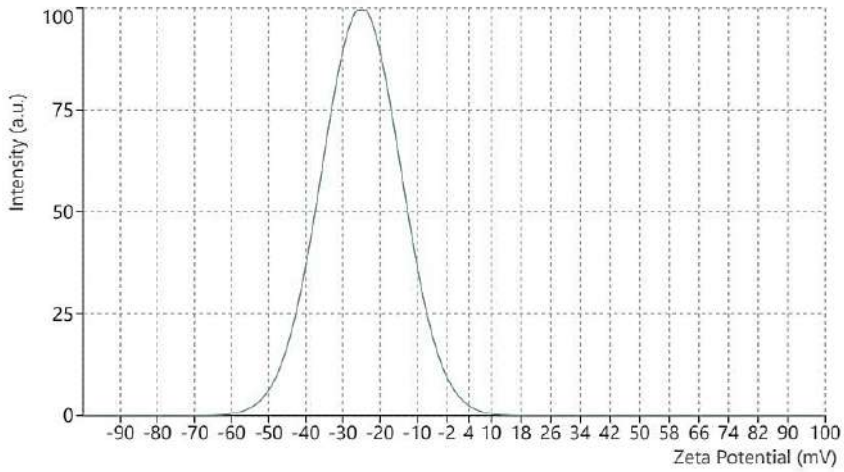

Figure 5: Zeta potential distribution of the synthesized Cu(II) complex.

The Zeta potential analysis reveals the following key features; Average Zeta Potential: The peak of the distribution is centered at approximately -25 mV, indicating that the Cu(II) complex particles carry a net negative surface charge in the measurement conditions. Distribution Width: The graph shows a relatively narrow, symmetrical distribution, suggesting a homogeneous surface charge across the particle population. The full width at half maximum (FWHM) of the peak is estimated to be about 30 mV, ranging from approximately -40 mV to -10 mV. Range: The Zeta potential values span from about -90 mV

to +100 mV, with the majority of the particles falling within the -60 mV to 0 mV range. Colloidal Stability: A Zeta potential of -25 mV indicates moderate colloidal stability. While this value suggests some electrostatic repulsion between particles, it falls within the range (-30 mV to +30 mV) where particles may have limited stability and could be prone to aggregation over time. Surface Chemistry: The negative Zeta potential suggests that the surface of the Cu(II) complex particles is dominated by anionic species or functional groups. This could be due to the nature of the ligands used in the complex formation or the adsorption of negative ions from the solution.

These Zeta potential findings complement our DLS observations by providing insights into the electrostatic properties of the particles in solution. The moderate negative charge helps explain the dispersion stability observed in the DLS measurements, as it provides some electrostatic repulsion between particles, preventing rapid aggregation. The relatively narrow distribution of Zeta potential values aligns with the homogeneity suggested by the DLS results, indicating consistent surface properties across the particle population. This uniformity is advantageous for applications requiring predictable particle-particle and particle-medium interactions. While the -25 mV Zeta potential suggests moderate stability, it may not be sufficient for long-term colloidal stability in all conditions. For applications requiring extended stability or dispersion in different media, surface modification strategies or the use of additional stabilizing agents might be considered to enhance the electrostatic or steric repulsion between particles.

The negative surface charge of the Cu(II) complex particles could influence their interaction with other charged species or surfaces. This property might be exploited in applications such as selective adsorption, catalysis, or in designing interfaces for sensors or electrochemical devices.

F. Antimicrobial Activity Assay

The antimicrobial activity of the synthesized Cu(II) complex was evaluated using the disk diffusion method against Escherichia coli. Figure 6 shows the inhibition zones observed on the agar plate, and Table 1 presents the measured inhibition zone diameters. Figure 7 provides a visual representation of the data in histogram form.

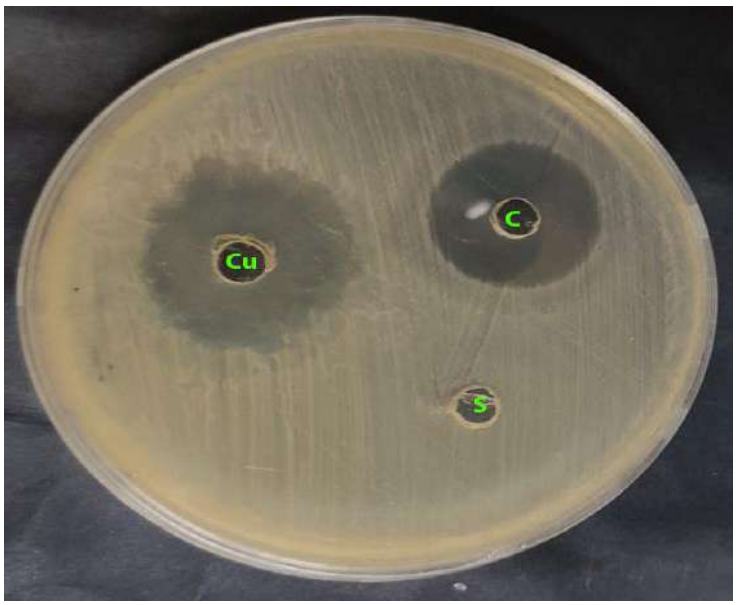

Figure 6: Inhibition zones of Cu(II) complex (Cu), control gentamicin (C), and solvent (S) against E. coli.

Table 1: Inhibition zone diameters for the Cu(II) complex, control, and solvent.

Sample	**Inhibition Zone Diameter (mm)**
Cu	18 ± 1
C	22 ± 1
S	0 ± 0

Cu = Cu complex, C = Control (Gentamicin), S = Solvent.

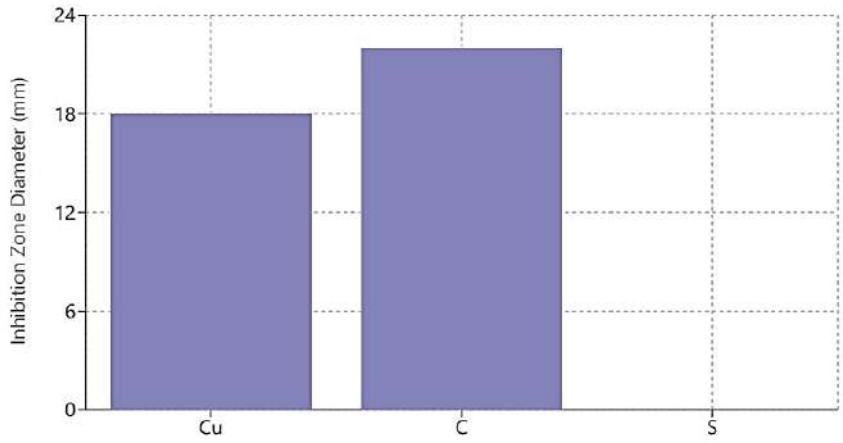

Figure 7: Histogram of inhibition zone diameters for the Cu(II) complex (Cu), control (C), and solvent (S).

The results of the antimicrobial activity assay reveal the following key observations; Cu(II) Complex Activity: The synthesized Cu(II) complex demonstrated significant antimicrobial activity against E. coli, with an average inhibition zone diameter of 18 ± 1 mm. This clear zone of inhibition indicates that the complex possesses potent antibacterial properties. Comparison with Control: The positive control, gentamicin (C), exhibited an inhibition zone of 22 ± 1 mm. The Cu(II) complex showed slightly less activity than the standard antibiotic, reaching approximately 82% of the control's efficacy. This suggests that the Cu(II) complex has strong antimicrobial potential, approaching the effectiveness of a clinically used antibiotic. Solvent Effect: The solvent (S) used to dissolve the Cu(II) complex showed no inhibition zone (0 ± 0 mm), confirming that the observed antimicrobial activity is solely due to the Cu(II) complex and not the solvent. Zone Characteristics: The inhibition zones for both the Cu(II) complex and gentamicin appear clear and well-defined, indicating complete inhibition of bacterial growth within these areas. The edges of the Cu(II) complex zone show a slight haziness, which might suggest a concentration-dependent effect or diffusion characteristics of the complex. Consistency: The small standard deviations in the measurements suggest good reproducibility of the antimicrobial effect across replicates.

The observed antimicrobial activity of the Cu(II) complex can be attributed to several potential mechanisms:

a) Reactive Oxygen Species (ROS) Generation: Cu(II) complexes are known to catalyze the production of ROS, which can cause oxidative stress and damage to bacterial cells.

b) DNA Interaction: The complex may interact with bacterial DNA, interfering with replication and transcription processes.

c) Protein Denaturation: Cu(II) ions can interact with sulfhydryl groups in proteins, leading to protein denaturation and bacterial cell death.

d) Membrane Disruption: The lipophilic nature of the complex may allow it to interact with and disrupt bacterial cell membranes.

The significant antimicrobial activity of the Cu(II) complex against E. coli, a gram-negative bacterium, is particularly noteworthy. Gram-negative bacteria are generally more resistant to antibiotics due to their additional outer membrane. The ability of the Cu(II) complex to effectively inhibit E. coli growth suggests its potential as a broad-spectrum antimicrobial agent.

However, the synthesized Cu(II) complex demonstrates promising antimicrobial activity against E. coli, warranting further investigation into its potential as a novel antimicrobial agent. These results, combined with the structural and physicochemical properties elucidated through XRD, SEM, AFM, DLS, and zeta potential analyses, provide a comprehensive characterization of this promising material.

IV. Conclusion

In conclusion, this study has successfully synthesized, characterized, and evaluated the antimicrobial properties of the novel copper(II) complex $[Cu(bpy)_2]Cl_2$. Through a comprehensive multi-technique approach, we have gained significant insights into the structural, physicochemical, and biological properties of this complex.

X-ray diffraction analysis revealed the precise crystal structure of $[Cu(bpy)_2]Cl_2$, confirming the coordination of two 2,2'-bipyridine ligands to the copper center. The diffraction pattern indicated a highly crystalline material with a unique structural arrangement. Jahn-Teller distortions, typical of Cu(II) complexes, were observed, providing valuable information about the electronic configuration and bonding within the complex.

Scanning Electron Microscopy (SEM) and Atomic Force Microscopy (AFM) analyses offered detailed insights into the morphology and surface characteristics of the complex. The observed layered structures and nanoscale features suggest a high surface area, which may contribute to the complex's reactivity and potential applications. The combination of these techniques provided a comprehensive view of the material's structure from the atomic to the microscale level.

Dynamic Light Scattering (DLS) measurements revealed that the complex forms nanostructures in solution with a mean hydrodynamic diameter of 45 nm. This finding has important implications for the complex's behavior in biological systems and solution-based applications. The narrow size distribution observed indicates a uniform assembly process, which is advantageous for potential catalytic or sensing applications.

Zeta potential analysis showed that the complex carries a net negative surface charge in solution, with a value of approximately -25 mV. This moderate negative charge explains the complex's colloidal stability and provides insights into its potential interactions with biological membranes and other charged species.

Crucially, the antimicrobial assay demonstrated significant activity of $[Cu(bpy)_2]Cl_2$ against Escherichia coli. The observed inhibition zone of 18 ± 1 mm indicates potent antibacterial properties, approaching the efficacy of the control antibiotic gentamicin. This finding is

particularly noteworthy given the increasing concern over antibiotic resistance and the need for new antimicrobial agents.

The antimicrobial activity of $[Cu(bpy)_2]Cl_2$ can be attributed to several potential mechanisms, including the generation of reactive oxygen species, DNA interaction, protein denaturation, and membrane disruption. The complex's ability to effectively inhibit E. coli, a gram-negative bacterium typically more resistant to antibiotics, suggests its potential as a broad-spectrum antimicrobial agent.

These results collectively demonstrate that $[Cu(bpy)_2]Cl_2$ is a promising candidate for further development as an antimicrobial agent. Its unique structural properties, combined with its potent antibacterial activity, open up new possibilities in the field of metal-based antimicrobials. This study contributes to the growing body of knowledge on copper-based coordination compounds and their potential applications in addressing the global challenge of antimicrobial resistance.

Furthermore, the comprehensive characterization of $[Cu(bpy)_2]Cl_2$ provides valuable insights into the relationship between the structure, physicochemical properties, and biological activity of copper(II) bipyridine complexes. This knowledge can inform the design and development of future metal-based functional materials and therapeutic agents.

However, this research not only advances our understanding of copper(II) bipyridine chemistry but also demonstrates the potential of such complexes in addressing real-world challenges like antimicrobial resistance. The findings pave the way for further investigations into the mechanisms of action, broader spectrum of antimicrobial activity, and potential applications of $[Cu(bpy)_2]Cl_2$ and related complexes in various fields, from materials science to medicinal chemistry.

References

[1] Turel I. Special issue: practical applications of metal complexes. Molecules. 2015 Apr 30;20(5):7951-6. doi: 10.3390/molecules20057951. PMID: 26007166; PMCID: PMC6272723.

[2] Ghosh SK. Diversity in the Family of Manganese Oxides at the Nanoscale: From Fundamentals to Applications. ACS Omega. 2020 Oct 5;5(40):25493-25504. doi: 10.1021/acsomega.0c03455. PMID: 33073076; PMCID: PMC7557223.

[3] Kaes, Christian & Katz, Alexander & Hosseini, Mir. (2000). Bipyridine: The Most Widely Used Ligand. A Review of Molecules Comprising at Least Two 2,2‘-Bipyridine Units. Chemical reviews. 100. 3553-90. 10.1021/cr990376z.

[4] Kilner CA, Halcrow MA. Change in electronic structure in a six-coordinate copper(II) complex accompanied by an anion order/disorder transition. Acta Crystallogr B. 2010 Apr;66(Pt 2):206-12. doi: 10.1107/S0108768110003678. Epub 2010 Mar 16. PMID: 20305354.

[5] Chandrakumar, Krs & Pal, Sourav. (2002). Study of Local Hard−Soft Acid−Base Principle to Multiple-Site Interactions. Journal of Physical Chemistry A - J PHYS CHEM A. 106. 10.1021/jp014499a.

[6] Krasnovskaya, O.; Naumov, A.; Guk, D.; Gorelkin, P.; Erofeev, A.; Beloglazkina, E.; Majouga, A. Copper Coordination Compounds as Biologically Active Agents. Int. J. Mol. Sci. 2020, 21, 3965. https://doi.org/10.3390/ijms21113965.

[7] Tapiero H, Townsend DM, Tew KD. Trace elements in human physiology and pathology. Copper. Biomed Pharmacother. 2003 Nov;57(9):386-98. doi: 10.1016/s0753-3322(03)00012-x. PMID: 14652164; PMCID: PMC6361146.

[8] Gao L, Zhang A. Copper-instigated modulatory cell mortality mechanisms and progress in oncological treatment investigations. Front Immunol. 2023 Aug 2;14:1236063. doi: 10.3389/fimmu.2023.1236063. PMID: 37600774; PMCID: PMC10433393.

[9] Surry DS, Buchwald SL. Diamine Ligands in Copper-Catalyzed Reactions. Chem Sci. 2010;1(1):13-31. doi: 10.1039/C0SC00107D. PMID: 22384310; PMCID: PMC3289286.

[10] Mohammadidehcheshmeh, Iman & Poursattar, Ahmad & Sadegh, Fatemeh & Soltani, Mohammad Ebrahim. (2024). Copper Application and Copper Nanoparticles in Chemistry. 10.5772/intechopen.1004068.

[11] Singh, R.; Singh, G.; George, N.; Singh, G.; Gupta, S.; Singh, H.; Kaur, G.; Singh, J. Copper-Based Metal–Organic Frameworks (MOFs) as an Emerging Catalytic Framework for Click Chemistry. Catalysts 2023, 13, 130. https://doi.org/10.3390/catal13010130.

[12] Zahn, Stefan & Reckien, Werner & Kirchner, Barbara & Staats, Holger & Matthey, Jens & Lützen, Arne. (2009). Towards Allosteric Receptors: Adjustment of the Rotation Barrier of 2,2 '-Bipyridine Derivatives. Chemistry (Weinheim an der Bergstrasse, Germany). 15. 2572-80. 10.1002/chem.200801374.

[13] Nemcsok, Denes & Wichmann, Karin & Frenking, Gernot. (2004). The Significance of π Interactions in Group 11 Complexes with N-Heterocyclic Carbenes. Organometallics. 23. 10.1021/om049802j.

[14] Haas KL, Franz KJ. Application of metal coordination chemistry to explore and manipulate cell biology. Chem Rev. 2009 Oct;109(10):4921-60. doi: 10.1021/cr900134a. PMID: 19715312; PMCID: PMC2761982.

[15] Constable, E.C.; Housecroft, C.E. Packing Motifs in [M(bpy)2X2] Coordination Compounds (bpy = 2,2′-bipyridine; X = F, Cl, Br, I). Crystals 2023, 13, 505. https://doi.org/10.3390/cryst13030505.

[16] May, Ann & Dempsey, Jillian. (2024). A new era of LMCT: leveraging ligand-to-metal charge transfer excited states for photochemical reactions. Chemical Science. 15. 10.1039/d3sc05268k.

[17] Kumagai H, Tamaki Y, Ishitani O. Photocatalytic Systems for CO2 Reduction: Metal-Complex Photocatalysts and Their Hybrids with Photofunctional Solid Materials. Acc Chem Res. 2022 Apr 5;55(7):978-990. doi: 10.1021/acs.accounts.1c00705. Epub 2022 Mar 7. PMID: 35255207; PMCID: PMC8988296.

[18] Crispini, Alessandra & Cretu, Carmen & Dreava, Diana & Andelescu, Adelina & Sasca, Viorel & Badea, Valentin & Aiello, Iolinda & Szerb, Elisabeta & Costisor, Otilia. (2017). Influence of the counterion on the geometry of Cu(I) and Cu(II) complexes with 1,10-phenanthroline. Inorganica Chimica Acta. 470. 10.1016/j.ica.2017.05.064.

[19] Sinha, N., & Wenger, O. S. (2023). Photoactive Metal-to-Ligand Charge Transfer Excited States in 3d6 Complexes with Cr0, MnI, FeII, and CoIII. Journal of the American Chemical Society, 145(9), 4903-4920. https://doi.org/10.1021/jacs.2c13432.

[20] Abdel Rahman, Afaf & Mahboub, Heba & Ezz-Eldin, Rasha & Abdelwarith, Dr: Abdelwahab & Younis, Elsayed & Khamis, Tarek & Aziz, Enas & Basha, Walaa & Elmaghraby, Ibrahim & Davies, Simon & Ismail, Sameh & Reyad, Yasmin. (2024). Lead toxicity in African catfish: Promising role of magnetite nanogel against etho-neurological alterations, antioxidant suppression, gene toxicity, and histopathological/ immunohistochemical disruptions. Aquaculture. 594. 741411. 10.1016/j.aquaculture.2024.741411.

[21] Youssef, Fady & Fouad, Omar & Ismail, Sameh & Mohamed, Gehad. (2024). Therapeutic and Toxicological Aspects of Some Metal Nanoparticles on The Central Nervous System: A Review. Egyptian Journal of Veterinary Sciences. 55. 733-745. 10.21608/ejvs.2023.234784.1609.

[22] Youssef, Fady & Fawzy, Heba & Ismail, Sameh & Mohamed, Gehad. (2024). The Role of Gold - Silver Nanocomposite Gel versus Astragalus Polysaccharides on Healing Process of Experimentally Induced Wound in Albino Rats Pharmacological and Histological Comparative Study. Egyptian Journal of Veterinary Sciences. 55. 803-816. 10.21608/ejvs.2023.247684.1668.

[23] Katowah, Dina & Ismail, Sameh & Alzahrani, Hanan & Rahman, Mohammed & Abd el-fadeel, Mohamed. (2024). Design of a novel nanosensor based on nanocomposite hydrogel composed of a PVA-poly(aniline-co-pyrrole) conducting copolymer-(PbO-doped NiO)-OXSWCNTs-coated QCM for rapid detection of cd (II) ions. Journal of Materials Science: Materials in Electronics. 35. 10.1007/s10854-024-12573-w.

[24] Al-Sodies, Salsabeel & Asiri, Abdullah M. & Ismail, Sameh & Alamry, Khalid & Hussein, Mahmoud. (2024). Development of poly(safranine-co-phenosafranine)/GNPs/MWCNTs nanocomposites for quartz crystal microbalance sensor detection of arsenic (III) ions. Materials Research Express. 11. 10.1088/2053-1591/ad37a5.

[25] Abdel Rahman, Afaf & Mahboub, Heba & Elshopakey, Gehad & Darwish, Mahmoud & Gharib, Heba & Shaalan, Mohamed & Fahmy, Esraa & Abdel-Ghany, Heba & Ismail, Sameh & Elsheshtawy, Hassnaa. (2024). Pseudomonas putida infection induces immune-antioxidant, hepato-renal, ethological, and histopathological/immunohistochemical disruptions in Oreochromis niloticus: the palliative role of titanium dioxide nanogel. BMC Veterinary Research. 127. 1-13. 10.1186/s12917-024-03972-6.

تخليق وتوصيف ونشاط مضاد للميكروبات لمركب.[Cu(bpy)2]Cl2

عثمان المجدوب السوسي[1]
فؤاد عبد الله جهان[2]
[1]كلية العلوم التقنية-قسم المواد العامة
[2]المعهد العالي للعلوم والتقنية- قسم التقنيات الكيميائية

استلمت الورقة بتاريخ ي/ش/س، وقبلت بتاريخ ي/ش/س، ونشرت بتاريخ ي/ش/س
الكلمات المفتاحية معقد النحاس الثنائي، 2,2'-بيبيريدين، البنية البلورية، الجسيمات النانوية، النشاط المضاد للميكروبات، الإشريكية القولونية.

استلمت الورقة بتاريخ 2025/02/02، وقبلت بتاريخ 2025/02/10 ونشرت بتاريخ 2025/02/12

الملخص

تناول هذه الدراسة تخليق وتوصيف شامل وتقييم مضاد للميكروبات لمركب نحاسي جديد**(II)** ، **[Cu(bpy)2]Cl2.**تم تصنيع المركب باستخدام إجراء معدّل يعتمد على تفاعل **CuCl2·2H2O**مع 2,2 **'-bipyridine.** تم توضيح الخصائص البنيوية والفيزيائية من خلال حيود الأشعة السينية**(XRD)** ، والمجهر الإلكتروني الماسح**(SEM)** ، والمجهر الذري للقوة **(AFM)**، والتشتت الضوئي الديناميكي**(DLS)** ، وتحليل جهد زيتا. كشف حيود الأشعة السينية عن بنية بلورية للغاية، بينما أظهر المجهر الإلكتروني الماسح والمجهر الذري للقوة **(AFM)** مورفولوجيا طبقية بخصائص نانوية. أشار **DLS** إلى متوسط قطر هيدروديناميكي يبلغ 45 نانومتر، وأشارت قياسات جهد زيتا إلى استقرار غرواني معتدل مع شحنة سطحية تبلغ -25 مللي فولت. أظهر المركب نشاطًا مضادًا للميكروبات بشكل كبير ضد الإشريكية القولونية، حيث أظهر منطقة تثبيط تبلغ 18 ± 1 مم، وهي مماثلة لمنطقة التحكم بالجنتاميسين (22 ± 1 مم). يُعزى هذا النشاط إلى آليات محتملة بما في ذلك توليد أنواع الأكسجين التفاعلية، وتفاعل الحمض النووي، وتحلل البروتين، وتدمير الغشاء. تشير النتائج إلى أن مركب **Cu(II)** هذا واعد كعامل مضاد للميكروبات جديد، مما يستدعي مزيدًا من التحقيق في قابلية تطبيقه الأوسع وآلية عمله.